Soft Actor-Critic Algorithm with Truly Inequality Constraint

Taisuke Kobayashi¹

Abstract—Soft actor-critic (SAC) in reinforcement learning is expected to be one of the next-generation robot control schemes. Its ability to maximize policy entropy would make a robotic controller robust to noise and perturbation, which is useful for real-world robot applications. However, the priority of maximizing the policy entropy is automatically tuned in the current implementation, the rule of which can be interpreted as one for equality constraint, binding the policy entropy into its specified target value. The current SAC is therefore no longer maximize the policy entropy, contrary to our expectation. To resolve this issue in SAC, this paper improves its implementation with a slack variable for appropriately handling the inequality constraint to maximize the policy entropy. In Mujoco and Pybullet simulators, the modified SAC achieved the higher robustness and the more stable learning than before while regularizing the norm of action. In addition, a real-robot variable impedance task was demonstrated for showing the applicability of the modified SAC to real-world robot control.

Index Terms—Reinforcement learning, Optimization and Optimal Control, Compliance and Impedance Control

I. INTRODUCTION

For the accomplishment of increasingly complex robot tasks (e.g. deformable object manipulation [1] and human-robot interaction [2]), data-driven control, especially (deep) reinforcement learning (RL) [3], is expected to be next-generation control scheme. Although learning had been limited to game environments and dynamics simulators, it has recently begun to be applied to real-world robot control and has illustrated outcomes [4]–[6].

One of the key players in this success is the state-ofthe-art learning algorithm, soft actor-critic (SAC) [7]. As its name suggests, SAC is a type of actor-critic algorithm, which is suitable for robot control because it allows control commands given in real numbers, such as joint torques. SAC renewed the learning law by adding maximization of policy entropy into the main objective of RL, which facilitates exploration while suppressing over-learning and improves learning quality and speed. In addition, as a side effect of the maximized policy entropy in its learning process, the policy can acquire the superior ability to recover from errors in various situations, which are encountered during the encouraged exploration [8], [9]. This ability corresponds to the robustness to noise and perturbation, which should be required for the real-world robot control as well as the control quality. Furthermore, various improvements have been proposed using SAC as a baseline: e.g. making SAC suitable for discrete action space [10]; improving the policy model

¹Taisuke Kobayashi is with National Institute of Informatics (NII) and with The Graduate University for Advanced Studies (SOK-ENDAI), 2-1-2 Hitotsubashi, Chiyoda-ku, Tokyo, 101-8430, Japan. kobayashi@nii.ac.jp

by combining normalizing flows [11] and; ensuring safety by considering the worst-case scenario [12]. Alternatively, SAC has been re-derived and analyzed in the context of control as inference [13].

One direction of improving SAC is the auto-tuning of the temperature parameter that determines the priority of the maximization of the policy entropy, which is added to SAC as an auxiliary objective. The most representative auto-tuning was developed by the authors who originally proposed SAC [8]. By reinterpreting SAC as a constrained optimization problem, the temperature parameter is given the meaning of a Lagrange multiplier, optimization procedure of which is applied to the temperature parameter. Popular libraries have implemented SAC with this function [14], [15], and empirically proven its simple and effective value, although its issue is raised later. Other methods have been studied, such as the use of meta-gradient [16] and the introduction of curiosity to further accelerate the exploration [17], but their improvement seems to be marginal.

Thus, SAC has been established as a modern standard RL algorithm, but as mentioned above, it is still in the process of improvement. In this study, the auto-tuning of the temperature parameter is modified. Specifically, this paper first points out that the current standard implementation can be regarded as an equality constraint on the policy entropy, which causes the policy entropy to converge to its lower bound without maximizing it [18]. In other words, the current auto-tuning of the temperature parameter would make SAC far from our expectation to maximize the policy entropy.

To resolve this issue, this paper introduces and optimizes a state-dependent slack variable for inequality constraint [19] to maximize the policy entropy so that it can appropriately be over a specified lower bound. In addition, since optimization of the slack variable becomes a multi-objective optimization, a switching-type scalarization instead of a simple weighted sum is introduced based on ϵ -insensitive loss [20]. This improvement is expected to appropriately yield the policy entropy maximization with the high robustness and alleviation of over-learning for more stability in the practical use.

The proposed method is validated on Mujoco [21] and Pybullet [22] simulators. The results show that the introduction of slack variable increases the policy entropy and improves the learning stability statistically. The entropy-maximized policy yields the higher robustness to adversarial situations while regularizing the norm of action. In addition, a real-robot variable impedance task is demonstrated for showing the applicability of the proposed method to real-world robot control.

II. PRELIMINARIES

A. Basic problem statement

RL [3] solves an optimal control problem that maximizes the sum of future rewards, so-called return. For this purpose, Markov decision process (MDP) is assumed with the tuple $(\mathcal{S}, \mathcal{A}, p_e, r)$ where \mathcal{S} and \mathcal{A} denote the state and action spaces, respectively, p_e gives the state transition probability, and r defines the reward at the current situation. Specifically, at the current state $s \in \mathcal{S}$ of an (unknown) environment, an agent decides its action $a \in \mathcal{A}$ according to its trainable policy $\pi(a \mid s)$ and interacts with the environment by a. As a result, s is updated to the next state s' according to the state transition probability $p_e(s' \mid s, a)$, while getting the reward r = r(s, a).

RL optimizes π to stochastically maximize the return obtained through interactions repeated from s at the current time step t, $R_t = \sum_{k=0}^{\infty} \gamma^k r(s_{t+k}, a_{t+k})$. For this optimization problem, RL often defines the following two types of value functions, which denote the expected values of R_t .

$$V(s) = \mathbb{E}_{\rho^{\pi}}[R_t \mid s], \ Q(s, a) = \mathbb{E}_{\rho^{\pi}}[R_t \mid s, a]$$
 (1)

where ρ^{π} denotes the probability to generate the state-action trajectory using π . Note that $V(s) = \mathbb{E}_{a \sim \pi}[Q(s,a)]$ holds in this standard case. Various learning algorithms have been proposed for learning these functions as well as π , and SAC, described below, is one of them. Note that, to learn π , V and/or Q, deep neural networks are widely used as function approximators of them. This paper also follows this popular way of implementation.

B. Soft actor-critic: SAC

Let's address SAC, which has achieved great success in recent years in RL and has become established as one of the standard methods [7]. Its main feature is that it solves the entropy-maximized problem by adding the policy entropy $\mathcal{H}(\pi) = \mathbb{E}_{\pi}[-\ln \pi]$ to the reward as follows:

$$r = r(s, a) + \alpha \mathcal{H}(\pi(\cdot \mid s)) \tag{2}$$

where $\alpha \geq 0$ denotes the temperature parameter to adjust the priority of the policy entropy.

According to this extension, the relationship between V and Q is first given as follows:

$$V(s) = \mathbb{E}_{a \sim \pi}[Q(s, a) - \alpha \ln \pi(a \mid s)] \tag{3}$$

With this, the soft Bellman equation derives the following bootstrapped supervised signal for Q as y.

$$Q(s, a) = r(s, a) + \gamma \mathbb{E}_{p_e(s'|s, a)}[V(s')]$$

$$= r(s, a) + \gamma \mathbb{E}_{p_e(s'|s, a), \pi(a'|s')}[Q(s', a') - \alpha \ln \pi(a' \mid s')]$$

$$= y$$
(4

It is known that Q can be correctly obtained as the expected value of the return by optimizing the approximated Q in order to satisfy this equality.

In the actual implementation of SAC, two different function approximators are prepared to approximate $Q_{1,2}$, which are utilized for avoiding overestimation of Q. In addition, the target networks $\bar{Q}_{1,2}$ [23] corresponding to them are provided to compute y. Therefore, learning of $Q_{1,2}$ is accomplished by solving the following minimization problem for temporal difference (TD) error.

$$Q_{1,2}^* = \arg\min_{Q_{1,2}} \mathbb{E}_{(s,a,s',r) \sim \mathcal{D}, a' \sim \pi} \left[\frac{1}{2} (y - Q_{1,2}(s,a))^2 \right]$$

$$y = r + \gamma \left\{ \min_{i=1,2} \bar{Q}_i(s',a') - \alpha \ln \pi(a' \mid s') \right\}$$
(5)

where $\mathcal{D} = \{(s, a, s', r)_i\}_{i=1}^N$ denotes the replay buffer of size N, in which the interaction data on MDP is stored as the tuple (s, a, s', r).

With the trained Q, π can be optimized to maximize V (or minimize -V) at any states as follows:

$$\pi^* = \arg\min_{\pi} \mathbb{E}_{s \sim \mathcal{D}}[-V(s)]$$

$$= \arg\min_{\pi} \mathbb{E}_{s \sim \mathcal{D}, a \sim \pi} \left[-\min_{i=1,2} Q_i(s, a) + \alpha \ln \pi(a \mid s) \right]$$
(6)

Here, by maximizing the smaller Q, a conservative update would be expected. This minimization problem can be solved using the reparameterization trick for $a \sim \pi$ [24].

Finally, how to automatically tune α , given as a constant parameter, is shown since its fine-tuning for each task is time consuming. This is a new definition in the literature written by the same authors of SAC [8]. Specifically, the optimization problem of SAC is first reinterpreted as a constrained optimization problem with respect to the policy entropy.

$$\pi^* = \arg\min_{\pi} \mathbb{E}_{s \sim \mathcal{D}, \rho^{\pi}} \left[-\sum_{k=0}^{\infty} \gamma^k r(s_{t+k}, a_{t+k}) \mid s \right]$$
 s.t.
$$\mathcal{H}(\pi(\cdot \mid s)) \ge \mathcal{H}^* \ (\forall s \in \mathcal{D})$$

where \mathcal{H}^* denotes the lower bound, which is often designed as $-|\mathcal{A}|$ for the continuous action space.

In that case, α is given as the Lagrange multiplier when reverting to the usual SAC optimization problem, and relying on this new interpretation, α can be optimized in the following minimization problem.

$$\alpha^* = \arg\min_{\alpha} \mathbb{E}_{s \sim \mathcal{D}, a \sim \pi} \left[-\alpha \left\{ \ln \pi(a \mid s) + \mathcal{H}^* \right\} \right] \quad (8)$$

Here, π in this problem should be π^* in theory, but since π^* is not given explicitly, it is substituted by π in practice. As a result, qualitatively, if $\ln \pi > \mathcal{H}^*$, α will be increased to maximize entropy; otherwise, if $\ln \pi < \mathcal{H}^*$, α will be decreased to allow smaller entropy. Note that, in order to satisfy $\alpha \geq 0$, $\tilde{\alpha} \in \mathbb{R}$ (e.g. $\alpha = e^{\tilde{\alpha}}$) is prepared as a trainable parameter and updated by using the mirror descent method [25].

III. PROPOSAL

A. Open issue in SAC

It has been reported that SAC acquires higher control performance (e.g. higher profitability and robustness) than previous RL algorithms. This is said to be mainly due to maximizing the policy entropy $\mathcal{H}(\pi)$. However, the actual implementation introduced in the above does not necessarily provide the maximal $\mathcal{H}(\pi)$.

This is because the auto-tuned temperature parameter α , as defined in eq. (8), only makes $\mathcal{H}(\pi)$ (or $-\ln \pi$) closer to \mathcal{H}^* , as expected from its qualitative behavior (also reported in the literature [18]). In other words, the above auto-tuning is regarded to be derived based on the method of Lagrange multiplier with equality constraint, which is inconsistent with the maximization of $\mathcal{H}(\pi)$. Therefore, even though the optimization problem was originally designed to maximize $\mathcal{H}(\pi)$ with *inequality* constraint, the implementation was for $\mathcal{H}(\pi) = \mathcal{H}^*$. Because of this behavior, \mathcal{H}^* is called target entropy, although it is defined as the lower bound. The limitation of $\alpha \geq 0$ may cause $\mathcal{H}(\pi) > \mathcal{H}^*$ without fully satisfying this equality constraint, but in practice, the autotuning makes $\mathcal{H}(\pi)$ converge to \mathcal{H}^* in the training (see the simulation results later). As a result, without an appropriate \mathcal{H}^* , the policy entropy is expected to be too small to achieve the expected performance, and the full fruits of maximizing the policy entropy to be obtained may not be appreciated.

B. Auto-tuned temperature with slack variable

To resolve this issue, this study transforms the troublesome inequality constraint into the simple equality constraint in another way. This allows the method of Lagrange multiplier to be used with the transformed equality constraint as in the conventional auto-tuning of α . For this purpose, a slack variable $\Delta \geq 0$ is commonly introduced [19] (even for the recent machine learning [26]).

$$\mathcal{H}(\pi(\cdot \mid s)) \ge \mathcal{H}^* \quad (\forall s \in \mathcal{D})$$

$$\Leftrightarrow \mathcal{H}(\pi(\cdot \mid s)) = \mathcal{H}^* + \Delta(s) \quad (\forall s \in \mathcal{D}, \ \Delta \ge 0) \quad (9)$$

In short, by finding Δ that holds $\mathcal{H}(\pi) - \mathcal{H}^* = \Delta$ at any states, the inequality constraint can be theoretically transformed into the equality constraint.

Given the appropriate Δ , the optimization of α improves from eq. (8) to the following one.

$$\alpha^* = \arg\min_{\alpha} \mathbb{E}_{s \sim \mathcal{D}, a \sim \pi} \left[-\alpha \left\{ \ln \pi(a \mid s) + \mathcal{H}^* + \Delta(s) \right\} \right]$$
(10)

As a simple interpretation of this update rule, α makes $-\ln \pi$ converge to $\mathcal{H}^* + \Delta \geq \mathcal{H}^*$, which is newly given as a target value (previously, \mathcal{H}^* was that role, not the lower bound of the policy entropy). In addition, since Δ is a state-dependent function, the different policy entropy for each state can be expected: for example, it may be small for scenes requiring accuracy and; large for scenes requiring exploration.

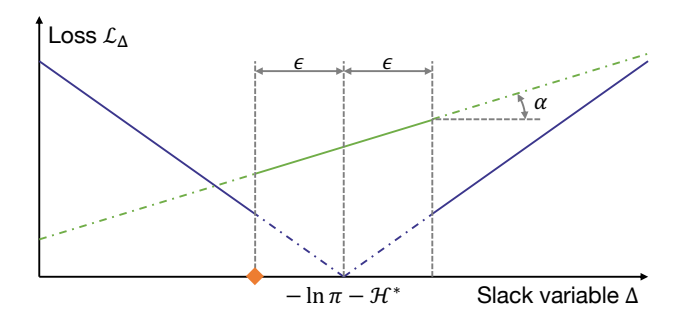


Fig. 1: Loss function for slack variable Δ

C. Optimization of slack variable

Now, Δ is specifically designed and optimized. Since Δ is state-dependent, it is first approximated by deep neural networks as well as π and $Q_{1,2}$. In the general slack variable, Δ is defined to be non-negative, and in the case of SAC, its upper bound is also found. That is, SAC mainly targets a bounded continuous action space, which is popular in many tasks, and explicitly transforms the action space so that $\mathcal{A}=(-1,1)^{|\mathcal{A}|}$. In such a box-constrained space, the policy can be uniformly distributed, $\pi=2^{-|\mathcal{A}|}$, with clearly maximal entropy. Similarly, even in a discrete action space, the uniform distribution, $\pi=|\mathcal{A}|^{-1}$, maximizes entropy.

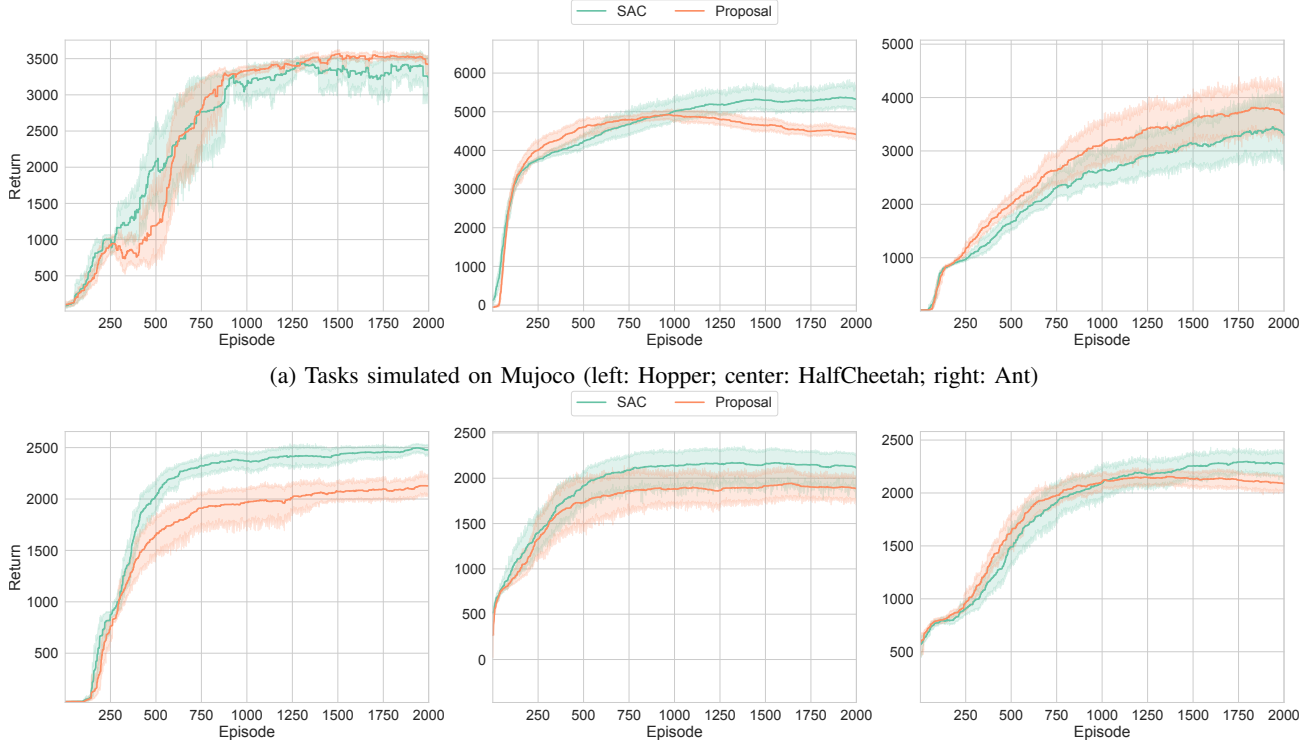
In summary, the upper bound of slack variable for the policy entropy in SAC, $\overline{\Delta}$, is obtained as follows:

$$\overline{\Delta} = \begin{cases} |\mathcal{A}| \ln 2 - \mathcal{H}^* & \text{(Continuous)} \\ \ln |\mathcal{A}| - \mathcal{H}^* & \text{(Discrete)} \end{cases}$$
 (11)

where \mathcal{H}^* for the continuous action space is recommended to be $-|\mathcal{A}|$ in the original paper [7] and \mathcal{H}^* for the discrete one is tuned as $0.98 \ln |\mathcal{A}|$ in SAC-Discrete [10]. Please note that \mathcal{H}^* has to be given such that $\overline{\Delta} \geq 0$. With $\overline{\Delta}$ and the fact that $\Delta \geq 0$, the real-valued output from the corresponding networks can be transformed to Δ within its domain properly by a sigmoid function and multiplying with $\overline{\Delta}$.

Then, the generated $\Delta \in [0, \overline{\Delta}]$ is optimized through minimization of an appropriate loss function. In general, Lagrangian function (a.k.a. the loss function for π in eq. (6)) should also be minimized with regard to Δ . In other words, $\alpha\Delta$ should be minimized for eliminating Δ , the speed of which depends on α , and for checking the performance on the edge (i.e. the lower bound). In particular, when α is small enough to allow $\mathcal{H}(\pi)$ to decrease, the decrease of Δ will be slowed down to moderate the decrease of $\mathcal{H}(\pi)$.

Another requirement is to minimize the error between the left and right sides of eq. (9). This can be done by minimizing the absolute error between the left and right sides of eq. (9), but if the equality constraint is sufficiently satisfied only by the optimization of Δ , the auto-tuning of α will not be achieved properly. To avoid this issue, ϵ -insensitive loss [20] is employed. That is, if the error is below a certain level $\epsilon \geq 0$, the optimization of Δ for satisfying the equality constraint is stopped.



(b) Tasks simulated on Pybullet (left: Hopper; center: HalfCheetah; right: Ant)

Fig. 2: Learning curves of the return R

Finally, it is necessary to set up a balance between the above two types of loss functions. The simple solution would be the weighted sum, but this would require the introduction and adjustment of a new weight hyperparameter. Instead of the weighted sum, a mechanism to switch between the two loss functions depending on ϵ is considered. That is, when the equality constraint is not achieved up to a certain level of ϵ , Δ is optimized only for satisfying the equality constraint, otherwise, Δ is gradually reduced to zero.

In summary, Δ is optimized through the following minimization problem.

$$\Delta^* = \arg\min_{\Delta} \mathbb{E}_{s \sim \mathcal{D}, a \sim \pi} [\mathcal{L}_{\Delta}(s, a; \epsilon)]$$
(12)
$$\mathcal{L}_{\Delta}(s, a; \epsilon) = \begin{cases} |\ln \pi(a \mid s) + \mathcal{H}^* + \Delta(s)| & \Delta(s) > \epsilon \\ \alpha \Delta(s) & \Delta(s) \le \epsilon \end{cases}$$

By minimizing this loss function, $\ln \pi + \mathcal{H}^* + \Delta = -\epsilon$ will be satisfied if $\ln \pi$ is stationary, as shown in Fig. 1. In practice, however, the equilibrium point is shifted by $\ln \pi$ according to the automatically tuned α , and Δ is optimized accordingly, which is an aspect of alternating optimization [27].

IV. EXPERIMENTS

A. Simulation conditions

Dynamical simulations are performed on Mujoco [21] and Pybullet [22] to verify the proposed SAC improvements. The tasks are *Hopper* (a.k.a. Hopper-v4 and HopperBulletEnv-v0), *HalfCheetah* (a.k.a. HalfCheetah-v4 and HalfCheetahBulletEnv-v0), and *Ant* (a.k.a. Ant-v4 and

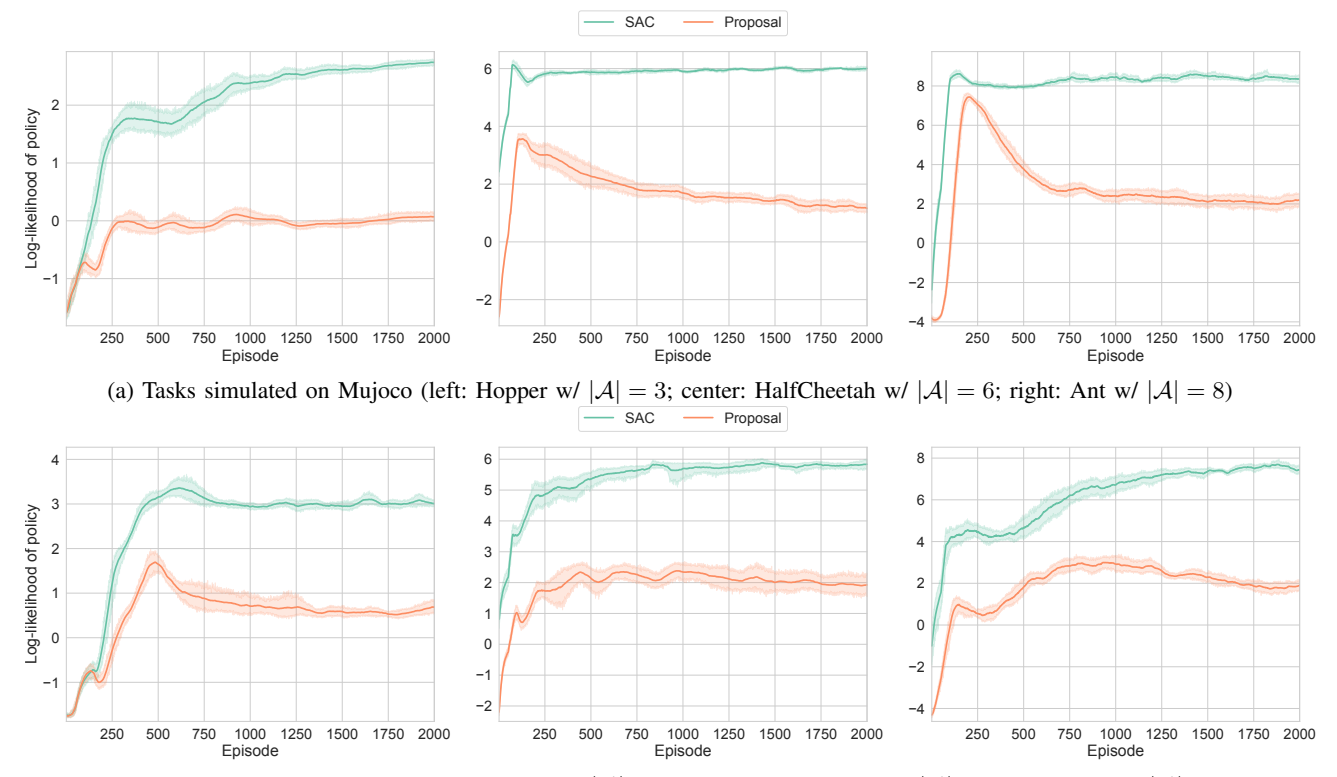
AntBulletEnv-v0) implemented on the respective simulators. To distinguish between the two simulators, the task names end with "M" for Mujoco "B" for Pybullet. Each task is trained for 2000 episodes and evaluated by the median of the return with 100 tests on the acquired policy. The learning results are statistically compared with 12 random seeds.

SAC is implemented in PyTorch [28], and the basic implementation follows the literature [23], [29]. As a small modification, RMSNorm [30] is introduced for the network normalization, instead of LayerNorm. Note that since Tanh function tends to concentrate the action near the boundary and its gradient tends to be large, an alternative transformation based on the literature [31], which has more stable gradients, is employed. This transformation is also utilized for the box constraint of $\Delta \in [0,\overline{\Delta}]$. As an optimizer, AdaTerm [32] with the default configurations is introduced.

As one of the hyperparameters, the initial value of α is set to 1. The lower bound of the policy entropy \mathcal{H}^* is set to $-|\mathcal{A}|$, which is originally recommended [8]. ϵ in eq. (12) is simply tuned to $\epsilon=0.05|\mathcal{A}|$ because all terms in the equality constraint on Δ are proportional to $|\mathcal{A}|$.

B. Learning tendency

The learning curves of the return R using the original SAC (labeled SAC) and the proposed method with the inequality constraint using the state-dependent slack variable (labeled Proposal) are depicted in Fig. 2. Note that they were obtained using the sampled actions from the policy during optimization of π . In addition, the episodic average of log-



(b) Tasks simulated on Pybullet (left: Hopper w/ $|\mathcal{A}|=3$; center: HalfCheetah w/ $|\mathcal{A}|=6$; right: Ant w/ $|\mathcal{A}|=8$)

Fig. 3: Learning curves of the log-likelihood of the policy $\ln \pi$ ($\mathcal{H}^* = -|\mathcal{A}|$)

likelihood of the policy $\ln \pi$ (corresponding to the negative policy entropy) is also shown in Fig. 3.

The results show that $\ln \pi$ in the original SAC is approximately stuck to $-|\mathcal{A}|$, and that the optimization of α satisfied the equality constraint for the lower bound \mathcal{H}^* . On the other hand, the proposed method clearly reduced $\ln \pi$ on average while allowing for fluctuation more, namely, made room for an increase in the policy entropy according to situations. The benefit of this increased policy entropy was confirmed in HopperM and AntM, where R was improved by suppressing over-learning. In addition, more efficient exploration can be found in HalfCheetahM and AntB, namely, the proposed method outperformed the original SAC in the early stages of learning. On the other hand, higher policy entropy inhibits deterministic actions. As a result, R tends to be worse for the tasks that require the deterministic action (HopperB and HalfCheetahB; and the later stages of learning for HalfCheetahM and AntB).

When the tasks were conducted with the deterministic actions of the learned policy, Fig. 4 was obtained. Note that R in this figure was normalized by the maximum and minimum of R obtained in each task. As can be seen in this figure, the proposed method outperformed or was comparable to the original SAC (except for HalfCheetahM). In particular, focusing on the worst-case scenario, the proposed method succeeded at a certain level in all trials, while the original SAC completely failed the tasks sometimes. Correspondingly, the variance in performance between trials was likely to be smaller for the proposed method.

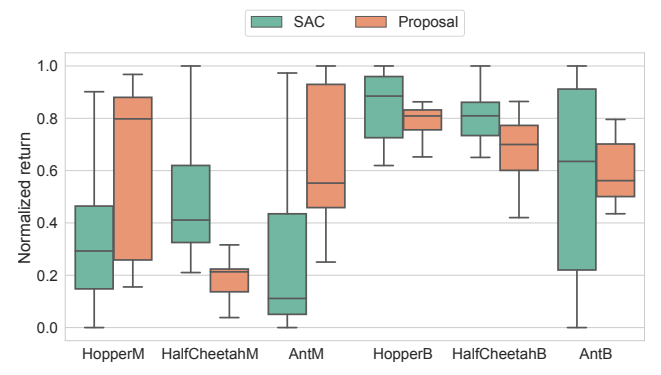


Fig. 4: Test results with the deterministic actions

C. Additional values of policy entropy maximization

Now, two other benefits of maximizing the policy entropy promoted by the proposed method are shown. First, SAC explicitly considers the bounded action space by transforming the non-bounded policy distribution, and as a result, the likelihood of actions near the boundary tends to be high. Therefore, maximizing the policy entropy leads to suppression of extreme action near the boundary. In fact, the magnitude of the actions as the normalized L2 norm, as illustrated in Fig. 5, shows that the proposed method made it smaller than the original SAC in all tasks. This contributes to suppressing over-learning, and from the viewpoint of robot control, it implicitly improves energy efficiency and smoothes out behaviors, as like the literature [29].

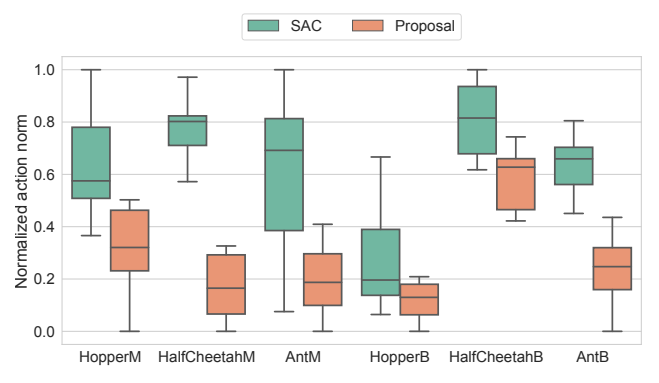


Fig. 5: Norm of the actions when testing the tasks

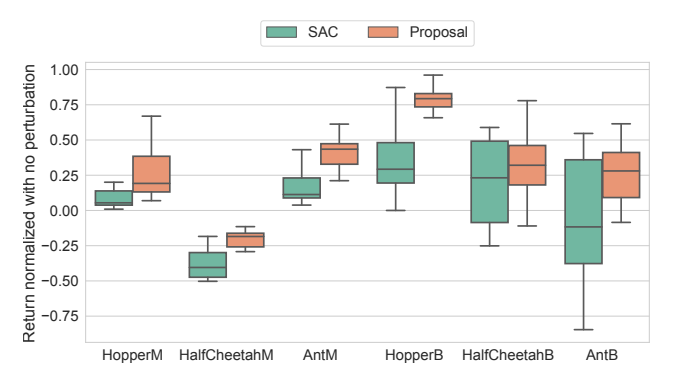


Fig. 6: Test results on the perturbed tasks

As a famous value of the entropy-maximized policy, the agent with it encountered various situations and learned how to recover from them. That is, the entropy-maximized policy is expected to be robust to perturbation, as suggested in the literature [8], [9]. To confirm such robustness, the learned policy was tested on the tasks with adversarial attacks, where the actions are replaced by ones generated from Gaussian noise and transformed within [-0.2, 0.2] with a probability of 5 % for Hopper and 20 % for others. As shown in Fig. 6, the proposed method outperformed the original SAC by still accomplishing the tasks robustly, while the original SAC suffered from significant performance degradation in most of tasks. In real-world robot control, various uncertainties and disturbing factors would be concerned, hence the robustness to them improves the reliability of the acquired policy.

D. Demonstrations with real robot

The usefulness of the proposed method in real-world robot control is demonstrated. The robot used in this experiment is a 5-DoF manipulator as shown in Fig. 7. When tracking a given trajectory for the robot's end-effector, six impedance parameters are optimized using RL as a variable impedance control system [33], [34]. This optimization aims to minimize efforts while keeping the trajectory error within a threshold. The details of the experimental configuration are summarized in Appendix A.

After training five models with different random seeds for each method, 10 different trajectories, which were not contained in the training phase, were evaluated with the



Fig. 7: Manipulator used in the variable impedance task

following criteria: i.e. return; tracking error; frequency of threshold exceeded; exerted effort; norm of action; and log-likelihood of policy. In order to show the performance improvement by training, the impedance parameters fixed to their initial values are also tested. In addition, to show the robustness of the policy trained by the proposed method, two cases are tested: *Weight*, where the end-effector grasped a weight (about 0.5 kg); and *Interaction*, where the target position of the end-effector was given passively while a human moved the end-effector through physical interaction. Note that the latter case was tested with four motion patterns, instead of the 10 trajectories.

Table I summarized the above test results, examples of which are shown in the attached video. First, both SAC and the proposed method on the same conditions as during training (a.k.a. Vanilla) outperformed the case with the fixed impedance parameters (a.k.a. Fixed) in terms of the return. This is due to the improvement of tracking accuracy, indicated in Tracking error and Threshold exceedance. Note that although the weight was grasped as an unknown disturbance, an offset to compensate for a shoulder-mounted gas spring was in fact insufficient, and therefore, the tracking accuracy was rather enhanced by the weight behaved as the additional compensation.

The behavior difference between SAC and the proposed method can be found from Table I. That is, in terms of the averaged tracking error, SAC and the proposed method were almost the same (although the proposed method slightly outperformed SAC) under all test conditions, but the proposed method clearly suppressed the frequency of threshold exceeded, which is directly related to reward, better than SAC. In addition, excepting the case with physical human-robot interaction (a.k.a. Interaction), the torque exerted was also better suppressed by the proposed method than by SAC. These results suggest that the proposed method can optimize the impedance parameters appropriately for situations in which the threshold is likely to be exceeded, while allowing for tracking error to some extent. This behavior can be regarded as a kind of worst-case optimization and implies

TABLE I: Test results of the variable impedance	task: the best in each test is written bold.
---	--

Test	Method	Criteria (SD)						
		Return	Tracking error	Threshold exceedance	Exerted effort	Action norm	Log-likelihood of policy	
		[-]	[m]	[%]	[Nm]	[-]	[–]	
Vanilla	Fixed	-0.93	0.036	5.09	3.47	N/A	N/A	
		(50.23)	(0.002)	(4.86)	(0.17)	N/A	N/A	
	SAC	23.34	0.032	2.61	3.62	1.76	6.16	
		(45.37)	(0.003)	(3.72)	(0.41)	(0.22)	(3.58)	
	Proposal	41.05	0.031	1.24	3.46	1.54	2.24	
		(18.64)	(0.002)	(1.58)	(0.17)	(0.29)	(3.70)	
Weight	SAC	37.70	0.022	0.27	4.19	1.72	5.83	
		(19.39)	(0.003)	(0.73)	(0.64)	(0.20)	(3.07)	
	Proposal	41.03	0.021	0.13	4.08	1.49	2.13	
		(16.75)	(0.003)	(0.50)	(0.54)	(0.34)	(4.04)	
Interaction	SAC	-29.85	0.032	6.34	9.61	1.80	7.12	
		(31.34)	(0.002)	(6.29)	(0.60)	(0.17)	(2.34)	
	Proposal	-14.64	0.031	3.29	9.86	1.61	3.35	
		(19.11)	(0.002)	(3.83)	(0.74)	(0.25)	(3.27)	

the high robustness of the proposed method. In fact, the proposed method performed better under the test conditions that differ from those in training. Note that the reason that the exerted torque by the proposed method exceeded by SAC may be due to the impedance parameters were adjusted to improve the tracking accuracy of the end-effector as part of this behavior, in preparation for the worst-case scenario from the large applied force.

Finally, the proposed method was able to suppress the norm of action and log-likelihood of the policy as well as in the simulations compared to SAC. This conservative learning tendency of the proposed method and its experience with a wide variety of impedance parameters during training would make the policy more robust to unknown test conditions, as described below.

V. CONCLUSION

This paper addressed the new auto-tuning way of the temperature parameter in SAC. Specifically, the previous method no longer maximizes the policy entropy, just constrains it to the target entropy. This is because the way of auto-tuning is interpreted as the derivation from equality constraint. To alleviate this issue, the desired inequality constraint to maximize the policy entropy was appropriately converted to the corresponding equality constraint using a state-dependent slack variable. In addition, the slack variable was optimized to satisfy the equality constraint while minimizing its value as much as possible. With the proposed improvement, the simulations on Mujoco and Pybullet verified the higher robustness to perturbation and the statistically more stable learning than the original SAC while regularizing the norm of action. Finally, usefulness of the robustness (and the conservative policy) was exemplified by a real-robot experiment.

However, in the absence of perturbations, the proposed method was sometimes inferior to the conventional SAC. A framework for adjusting the lower bound \mathcal{H}^* , as in the literature [18], or a more theoretically valid lower bound should be investigated in the near future.

APPENDIX

A. Experimental configuration

For the variable impedance task, a 5-DoF manipulator as shown in Fig. 7 is used. It consists of actuators (and frames) developed by HEBI Robotics, and each actuator is a series elastic actuator (SEA). Therefore, The torque exerted can be calculated from the difference in rotation angles before and after its internal spring, and torque control is available accordingly. In the experiment, only the official controllers provided by HEBI Robotics were used: i.e. control strategy 4 to the target position and velocity; a gravity compensation; an offset to roughly compensate for the shoulder-mounted gas spring; and a task-space impedance controller with virtual spring and damper for each axis. The PID gain is set lower than the default so that tracking errors are intentionally encountered, and the compensation by the impedance controller contributes to the performance.

For this manipulator, the following sine wave is given as the target trajectory of its end-effector.

$$p^{\text{tar}}(t) = p^{\text{ini}} \pm A \sin(\omega \pi t) \tag{13}$$

where t denotes the elapsed time from the beginning of episode (with 20 ms control period) and $p^{\rm ini}$ is given by the forward kinematics for the center of each joint range as the initial position of the end-effector. A denotes the amplitude for each axis: $A_{xy} \in [0.05, 0.15]^2$ for horizontal plane and; $A_z \in [0.01, 0.05]$ for vertical direction. $\omega \in [0.1, 1]^3$ for all axes are given as the axis-dependent frequency. A, ω , and the sign \pm are uniformly randomized independently during each episode. To track $p^{\rm tar}$, the target joint angle $q^{\rm tar}$ and velocity $\dot{q}^{\rm tar}$ are computed using the inverse kinematics [35], sending to each actuator as a command.

Under the above impedance control system for tracking the given trajectory, RL (i.e. SAC and the proposed method) optimizes the impedance parameters (i.e. three-dimensional virtual spring $k_p \in [0,100]^3$ and damper $k_d \in [0,10]^3$). To this end, action space is designed as their variations (i.e. six dimensions in total), which are restricted to ± 5 % of the maximum. The following reward function is given to

track the target trajectory within an allowable error while minimizing effort.

$$r = \exp\left(-\sum_{i} |\tau_{i}|\right) - \begin{cases} 1 & \|p^{\text{tar}} - p^{\text{obs}}\|_{2} > 0.05\\ 0 & \text{otherwise} \end{cases}$$
(14)

where τ denotes the efforts of actuators, $p^{\rm obs}$ is computed by the forward kinematics for the observed angles as the observed end-effector position. In order for RL to satisfy MDP with these configurations, the state space is given as a total of 32 dimensions consisting of the angle, angular velocity, effort, and temperature for each actuator; the observed and target positions of the end-effector; and the current impedance parameters.

ACKNOWLEDGMENT

This work was supported by JST, PRESTO Grant Number JPMJPR20C3, Japan.

REFERENCES

- Y. Tsurumine, Y. Cui, E. Uchibe, and T. Matsubara, "Deep reinforcement learning with smooth policy update: Application to robotic cloth manipulation," *Robotics and Autonomous Systems*, vol. 112, pp. 72–83, 2019
- [2] T. Kobayashi, E. Dean-Leon, J. R. Guadarrama-Olvera, F. Bergner, and G. Cheng, "Whole-body multicontact haptic human-humanoid interaction based on leader-follower switching: A robot dance of the "box step"," Advanced Intelligent Systems, p. 2100038, 2021.
- [3] R. S. Sutton and A. G. Barto, Reinforcement learning: An introduction. MIT press, 2018.
- [4] O. M. Andrychowicz, B. Baker, M. Chociej, R. Jozefowicz, B. Mc-Grew, J. Pachocki, A. Petron, M. Plappert, G. Powell, A. Ray et al., "Learning dexterous in-hand manipulation," *The International Journal of Robotics Research*, vol. 39, no. 1, pp. 3–20, 2020.
- [5] B. Osiński, A. Jakubowski, P. Zięcina, P. Miłoś, C. Galias, S. Homoceanu, and H. Michalewski, "Simulation-based reinforcement learning for real-world autonomous driving," in *IEEE International Conference on Robotics and Automation*. IEEE, 2020, pp. 6411–6418.
- [6] Z. Li, X. Cheng, X. B. Peng, P. Abbeel, S. Levine, G. Berseth, and K. Sreenath, "Reinforcement learning for robust parameterized locomotion control of bipedal robots," in *IEEE International Conference* on Robotics and Automation. IEEE, 2021, pp. 2811–2817.
- [7] T. Haarnoja, A. Zhou, P. Abbeel, and S. Levine, "Soft actor-critic: Off-policy maximum entropy deep reinforcement learning with a stochastic actor," in *International conference on machine learning*. PMLR, 2018, pp. 1861–1870.
- [8] T. Haarnoja, A. Zhou, K. Hartikainen, G. Tucker, S. Ha, J. Tan, V. Kumar, H. Zhu, A. Gupta, P. Abbeel, and S. Levine, "Soft actorcritic algorithms and applications," arXiv preprint arXiv:1812.05905, 2018.
- [9] B. Eysenbach and S. Levine, "Maximum entropy rl (provably) solves some robust rl problems," in *International Conference on Learning Representations*, 2021.
- [10] P. Christodoulou, "Soft actor-critic for discrete action settings," arXiv preprint arXiv:1910.07207, 2019.
- [11] P. N. Ward, A. Smofsky, and A. J. Bose, "Improving exploration in soft-actor-critic with normalizing flows policies," arXiv preprint arXiv:1906.02771, 2019.
- [12] Q. Yang, T. D. Simão, S. H. Tindemans, and M. T. Spaan, "Wesac: Worst-case soft actor critic for safety-constrained reinforcement learning," in *Proceedings of the AAAI Conference on Artificial Intelligence*, vol. 35, no. 12, 2021, pp. 10639–10646.
- [13] S. Levine, "Reinforcement learning and control as probabilistic inference: Tutorial and review," arXiv preprint arXiv:1805.00909, 2018.
- [14] E. Liang, R. Liaw, R. Nishihara, P. Moritz, R. Fox, K. Goldberg, J. Gonzalez, M. Jordan, and I. Stoica, "Rllib: Abstractions for distributed reinforcement learning," in *International Conference on Machine Learning*. PMLR, 2018, pp. 3053–3062.

- [15] A. Raffin, A. Hill, A. Gleave, A. Kanervisto, M. Ernestus, and N. Dormann, "Stable-baselines3: Reliable reinforcement learning implementations," *Journal of Machine Learning Research*, vol. 22, no. 268, pp. 1–8, 2021.
- [16] Y. Wang and T. Ni, "Meta-sac: Auto-tune the entropy temperature of soft actor-critic via metagradient," arXiv preprint arXiv:2007.01932, 2020
- [17] J. Lin, C. Huang, X. Liang, and L. Lin, "Cat-sac: Soft actor-critic with curiosity-aware entropy temperature," 2020.
- [18] Y. Xu, D. Hu, L. Liang, S. McAleer, P. Abbeel, and R. Fox, "Target entropy annealing for discrete soft actor-critic," arXiv preprint arXiv:2112.02852, 2021.
- [19] S. Boyd, S. P. Boyd, and L. Vandenberghe, Convex optimization. Cambridge university press, 2004.
- [20] V. Vapnik, The nature of statistical learning theory. Springer science & business media, 1999.
- [21] E. Todorov, T. Erez, and Y. Tassa, "Mujoco: A physics engine for model-based control," in *IEEE/RSJ International Conference on Intelligent Robots and Systems*. IEEE, 2012, pp. 5026–5033.
- [22] E. Coumans and Y. Bai, "Pybullet, a python module for physics simulation for games, robotics and machine learning," *GitHub repository*, 2016
- [23] T. Kobayashi, "Consolidated adaptive t-soft update for deep reinforcement learning," arXiv preprint arXiv:2202.12504, 2022.
- [24] D. P. Kingma and M. Welling, "Auto-encoding variational bayes," in International Conference on Learning Representations, 2014.
- [25] A. Beck and M. Teboulle, "Mirror descent and nonlinear projected subgradient methods for convex optimization," *Operations Research Letters*, vol. 31, no. 3, pp. 167–175, 2003.
- [26] V. Picheny, R. B. Gramacy, S. Wild, and S. Le Digabel, "Bayesian optimization under mixed constraints with a slack-variable augmented lagrangian," *Advances in neural information processing systems*, vol. 29, 2016.
- [27] J. C. Bezdek and R. J. Hathaway, "Convergence of alternating optimization," *Neural, Parallel & Scientific Computations*, vol. 11, no. 4, pp. 351–368, 2003.
- [28] A. Paszke, S. Gross, S. Chintala, G. Chanan, E. Yang, Z. DeVito, Z. Lin, A. Desmaison, L. Antiga, and A. Lerer, "Automatic differentiation in pytorch," in *Advances in Neural Information Processing* Systems Workshop, 2017.
- [29] T. Kobayashi, "L2c2: Locally lipschitz continuous constraint towards stable and smooth reinforcement learning," in *IEEE/RSJ International Conference on Intelligent Robots and Systems*, 2022, pp. 4032–4039.
- [30] B. Zhang and R. Sennrich, "Root mean square layer normalization," Advances in Neural Information Processing Systems, vol. 32, 2019.
- [31] J. T. Barron, "Squareplus: A softplus-like algebraic rectifier," arXiv preprint arXiv:2112.11687, 2021.
- [32] W. E. L. Ilboudo, T. Kobayashi, and M. Takamitsu, "Adaterm: Adaptive t-distribution estimated robust moments towards noise-robust stochastic gradient optimizer," arXiv preprint arXiv:2201.06714, 2022.
- [33] J. Buchli, F. Stulp, E. Theodorou, and S. Schaal, "Learning variable impedance control," *The International Journal of Robotics Research*, vol. 30, no. 7, pp. 820–833, 2011.
- [34] F. Ficuciello, L. Villani, and B. Siciliano, "Variable impedance control of redundant manipulators for intuitive human–robot physical interaction," *IEEE Transactions on Robotics*, vol. 31, no. 4, pp. 850–863, 2015.
- [35] T. Kobayashi, "Mirror-descent inverse kinematics for box-constrained joint space," arXiv preprint arXiv:2101.07625, 2021.